PHYSICAL REVIEW B VOLUME 16, NUMBER 12 15 DECEMBER 1977

Phonon spectroscopy. II. Spectral, spatial, and temporal evolution of a phonon pulse*

W. E. Bron and W. Grill
Department of Physics, Indiana University, Bloomington, Indiana 47401
(Received 9 June 1977)

A vibronic sideband spectrometer has been used to determine the spectral, spatial, and temporal evolution of a phonon distribution propagating in a crystal of SrF_2:Eu^{2+}. Spectral and spatial evolution depends strongly on the frequency dependence of phonon scattering at the Eu^{2+} probe ions. The mean free path of phonons in the frequency range of 1–4 THz is found to vary from 10^{-3} to 10^{-4} mm. The temporal evolution is strongly influenced by anharmonic processes. The effective lifetime for phonons of frequency from 1 to 3 THz is found to be of the order of microseconds.

I. INTRODUCTION

In the preceding paper[1] we report the application of a vibronic-sideband spectrometer to the spectral resolution of a phonon distribution which crosses an interface between a "heater" film and a crystal. In the present paper we use the spectrometer to determine the spectral, spatial, and temporal evolution of the phonon distribution as it propagates inside a crystal of SrF_2:Eu^{2+}. The following functional dependences are determined:

(i) The differential spectral distribution function $\Delta n_{x,t}(\omega)$, measured at a fixed distance into the crystal x, and at fixed time t. The observation volume differs from the integrating volume used in Ref. 1. Here the volume is defined by the laser beam used to excite the luminescence of the Eu^{2+} probe ions inside the crystal. (We refer to this volume as the focal volume or focal column.)

(ii) The change as a function of distance into the crystal of the number of phonons in a small frequency interval about the frequency ω at a fixed time. We denote the spatial evolution, when normalized to the phonons present in the focal column placed immediately behind the interface, i.e., at $x=0$, as $N_{t,\omega}(x)$.

(iii) The change in the number of phonons of a given frequency as a function of time, normalized to the phonons present at $t=0$, as the phonons propagate inside an integrating volume, $\bar{v}$ (larger than the focal volume) of the SrF_2 crystal. We shall refer to this aspect of the temporal evolution as $\bar{N}_{x,\omega}(t)$.

(iv) $\Delta N_{x,\omega}(t)$, the change in the differential vibronic sideband amplitude as a function of time as observed, at fixed phonon frequencies, from the luminescence of the focal column fixed in position inside the crystal.

The spectral distribution of phonons propagating in crystal systems has been previously measured by other means as have the spatial and temporal evolution of fixed, single-frequency components of a phonon distribution.[2] To our knowledge no previously reported technique permits measurements of all three propagation parameters. The present experiment includes observations on phonons with frequency up to 6 THz.

In an earlier paper[3] we have discussed the characteristics of the phonon transport in SrF_2:Eu^{2+}. It was found that the Eu^{2+} probe ions act as scattering centers which hinder the free flow of phonons. The frequency dependence of the scattering process was predicted using a T-matrix scattering formalism and a shell-model representation of the lattice dynamics of pure SrF_2. Two major simplifying assumptions are incorporated in these calculations. The first is that the disturbance matrix, which contains the effective changes in the dynamical parameters due to the presence of the probe ions, can be described by the difference in these parameters between the SrF_2 and EuF_2 pure lattices. The second simplification is to neglect shell polarization in the calculation of the scattering probability. The latter assumption, which is normally made in calculations of this type, is actually only applicable in the long-wavelength limit and is likely to break down for phonon frequencies above 1–2 THz. The calculated relative scattering probability determined in this way for the entire one-phonon frequency interval appears as Fig. 2 of Ref. 3.

It was also possible to determine experimentally the relative scattering probability using superconducting "fluorescence"[4] as a source of quasimonochromatic phonons at 287, 407, and 670 GHz. The experimental methods were, however, too crude to afford a critical comparison between the results and the scattering formalism. Only qualitative agreement between experiment and theory was indicated. Among the conclusions

to be drawn from the previous work is that the frequency dependence of the scattering probability depends on various in-band scattering resonances and does not vary as ω^4 as is usually assumed,[5] so that it is unlikely that high-frequency phonon transport in this system can be inferred from the transport behavior below 1 THz.

Phonon-phonon interactions also influence the experimental observations. The original phonon population in a given small frequency interval will change in time. The number of phonons in the interval will change through: (i) the decay of phonons originally in the interval; (ii) repopulation through the decay of higher-frequency phonons; and (iii) repopulation through recombinations of two or more lower-frequency phonons.

II. EXPERIMENTAL TECHNIQUE

The experimental apparatus and techniques outlined in Ref. 1 are adapted to determine the quantities listed in Sec. I. In order to measure $\bar{N}_{x,\omega}(t)$ the focal column of the N_2 laser is repetitively linearly swept over a volume $\bar{v}$ to achieve an integration over a distance of 0.4 mm in all directions from the interface. As will be demonstrated in Sec. IV, this distance is sufficient so that no more than 10% of all phonons of frequency greater than 3 THz entering the volume from the film-crystal interface can escape the volume over a time interval of 2 μsec. The duration of the observation gate on the photomultiplier tube output is made short compared to any variation in the signal, but not shorter than 100 nsec. The onset of the gate is scanned from $t=0$ to $t=4$ μsec relative to the onset of the voltage pulse across the heater film. The quantity $N_{x,\omega}(t)$ is measured in an analogous manner. The differential distribution function $\Delta n_{x,t}(\omega)$ is measured in the same way as $\Delta n(\omega)$ of Ref. 1 except that the observation volume is limited to the focal volume of the laser beam.

The signal amplitude as a function of distance into the crystal is measured by displacing mechanically the focal volume from a position which overlaps the film-crystal interface through a distance of 2.5 mm into the crystal. $N_{t,\omega}(x)$ is then obtained by normalization to the signal amplitude at $x=0$. In this connection it is important to note that the laser beam is not necessarily uniform over its cross section. The focused beam has roughly a Gaussian profile with a cross-sectional diameter (at half maximum amplitude) of 0.1 mm. Moreover, a weak superradiance is observed in the laser discharge. In addition, the surface of the crystal which contains the interface is not perfectly flat. These factors limit the resolution of the measurements. All other experimental parameters have been described in Ref. 1.

It is important to recall from Ref. 1 that all crystal surfaces have been carefully polished and that the crystal is placed in vacuum except for one surface which is in contact with liquid helium. Low-frequency phonons are, accordingly, expected to be spectrally reflected at the free surfaces although this may not be the case for high-frequency phonons. The time for the crystal to return to the temperature of the helium bath after the injection of a phonon pulse is experimentally observed to be of the order of 10^{-4} sec.

The experimental results described in Sec. III are obtained from phonon distributions generated by pulsing the constantan film with 500 V, i.e., at 5×10^3 W/mm^2, for a duration of 20 nsec.

III. EXPERIMENTAL RESULTS AND ANALYSIS

A. Spectral distribution

The differential spectral distribution function $n_{x,t}(\omega)$, as determined for various input powers, is displayed in Fig. 1. A detailed comparison of these results with those displayed in Fig. 4 of Ref. 1 show that the ratio of the concentration of low-frequency phonons (<1 THz) to high-frequency phonons is less in the focal volume than in the integrating volume.

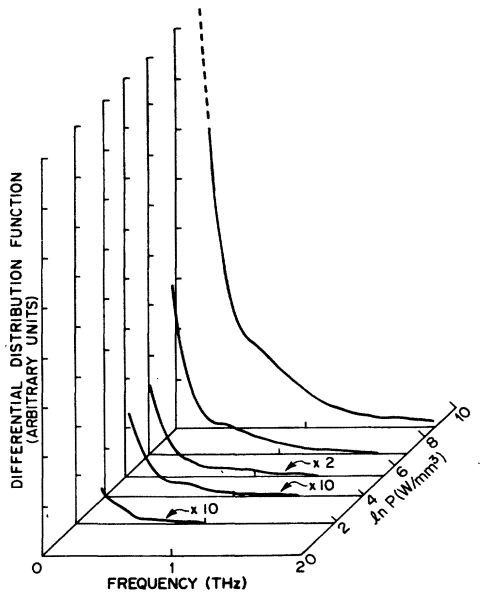

FIG. 1. Differential spectral distribution function $\Delta n_{x,t}(\omega)$, as measured in the focal volume for various input powers P. Note that the function for each of the lowest three input powers has been scaled up.

The origin of this effect lies in the frequency dependence of the scattering at the Eu^{2+} probe ions. Low-frequency phonons are not as strongly scattered as are high-frequency phonons and, accordingly, pass from the focal volume into the rest of the crystal in a shorter period of time. The defect scattering serves to constantly segregate low- from high-frequency phonons in any small region of the crystal. It is this process which makes it impossible to form a second sound pulse[6] in a medium containing strong scattering sites.

B. Spatial evolution

The difference in the scattering strength between low- and high-frequency phonons is most clearly demonstrated in the observed spatial evolution $N_{t,\omega}(x)$. The experimental results are shown as solid lines in Fig. 2. The more strongly scattered high-frequency phonons have a shorter mean free path and hence, after a given time period, have penetrated shorter distances into the crystal than have low-frequency phonons. The stronger the scattering probability the more nearly is the phonon transport purely diffusive. In contrast, the lower the phonon frequency, the longer the mean free path and the smaller is the mean number of scattering events required to cover a given distance, until at the limit of a very low frequency the transport becomes purely ballistic.

In the diffusive regime, the relative number of phonons which after a time t have traveled a distance z between a column generator and a column detector, both of length l, is given by the relation[7]

$$W(z,t) = \pi^{-3/2}(4Dt)^{-1/2}(1 - e^{-l^2/4Dt})\, e^{-z^2/4Dt}, \quad (1)$$

in which D is the diffusion constant. The dotted portions of each curve in Fig. 2 represents the least-square-deviation fit to three-dimensional diffusion between the column heater film and the focal column detector. (The difference between the experimental and fitted results in the upper portion of the curves is too small to be shown in Fig. 2.) It is clear that at frequencies between 1 and 4 THz processes other than pure diffusion are present to varying degree. No meaningful fit to a diffusion profile could be achieved for 0.5 THz phonons. In the latter case the spatial evolution is controlled by the high-frequency phonons which are congregated near the interface from whence, over long periods of time, they emit by decay low-frequency phonons which travel nearly ballistically.

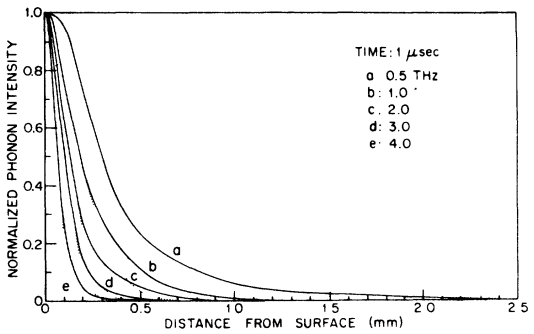

FIG. 2. Spatial evolution $N_{t,\omega}(x)$, normalized to the signal at $x=0$. The solid lines are the spatial profiles, for various phonon frequencies, as determined after 1 μsec has elapsed. The dotted lines are part of a least-square fit to a Gaussian profile. The fitted curve to the upper portions of the profile has been omitted because the deviations from the experimental curve are too small.

In Table I are listed the diffusion constants obtained from the fitting procedure. The scattering rates and mean free paths are obtained from the diffusion constants on the further assumption that the phonons travel, between scattering events, at the weighted average acoustic velocity. The experimental results are compared to those predicted by the T-matrix formalism [see Eq. (1) of Ref. 3]. Although the calculated and experimental values are within an order of magnitude of each other the frequency dependence differs

TABLE I. Diffusion parameters.

Frequency (THz)	1.0	2.0	3.0	4.0
Experimental diffusion constant ($mm^2\ sec^{-1}$)	18.7×10^3	8.2×10^3	4.8×10^3	1.8×10^3
Experimental scattering rate (sec^{-1})	2.4×10^8	5.5×10^8	9.5×10^8	2.5×10^9
Calculated scattering rate (sec^{-1})	2.4×10^9	6.8×10^9	3.8×10^8	2.1×10^{10}
Experimental mean free path (mm)	15.0×10^{-3}	7.0×10^{-3}	4.0×10^{-3}	1.0×10^{-3}

markedly. We leave to a future investigation to determine whether or not the discrepancy can be rectified by including shell polarization in the dynamical matrix of the scattering formalism and/or by modification of the dynamical parameters in the vicinity of the probe ion.

C. Phonon decay

The temporal evolution of the phonon pulse as measured in the integrating volume $\bar{v}$, of the crystal at fixed frequencies, i.e., $\bar{N}_{x,\omega}(t)$, is displayed in Fig. 3. The data confirm the generally expected result that high-frequency phonons decay more rapidly than lower-frequency phonons. Since the curves at each frequency are not straight lines, no single, simple relaxation time can be assigned to the decay process. Nor, for that matter, are simple decay processes expected since, as already noted in Sec. I, each frequency interval is being repopulated by varying amounts and at varying times through the decay of high-frequency phonons and through the combination of low-frequency phonons.

Although no single decay time can be extracted from the data, a rough value for 3-THz phonons is obtained in the following manner. The experimental observation is the superposition of the following processes: (i) the decay of 3-THz phonons; (ii) the repopulation of 3-THz phonons through the decay of higher frequency phonons; (iii) the repopulation of 3-THz phonons through combinations of two or more low-frequency phonons; (iv) the escape of 3-THz phonons from the observation volume. We show that processes (ii) and (iii) occur over sufficiently different time intervals, such that the result in the time interval from approximately 1–3 μsec represents only processes (i) and (iii).

From measurements of the spectral distribution as a function of time after the heat pulse, it is known that after ~1 μsec the sum of all phonons of frequency greater than ~3.5 THz is less than those in the 3-THz observation interval. Accordingly, after this time the repopulation from the decay of high-frequency phonons into the 3-THz population should be small. Measurements of the spatial evolution of the pulse, after different elapsed times, show that beyond 3 μsec 10% of the 3-THz phonons have escaped the observation volume.[8] The change in the signal between these limits should represent the net result of the loss of phonons out of the 3-THz interval and the gain into the interval by combinations of low-frequency phonons. The value of the slope in the range from 1 to 3 μsec leads to an average relaxation time of 1.5 μsec.

Finally, note should be taken that no appreciable change in phonon number occurs at any frequency in the time interval $0<t<300$ nsec. It is for this reason that $\Delta n(\omega)$ of Ref. 1 was observed within this time interval.

D. Time resolution

The differential sideband amplitude as a function of time, $\Delta N_{x,\omega}(t)$, i.e., the evolution of a fixed frequency component of the phonon pulse as a function of time as measured at a fixed displacement from the interface, is displayed in Fig. 4. The zero in time has been displaced relative to the onset of the heat pulse by an amount (19 nsec) equal to the transit time for a longitudinal phonon, traveling at the sound velocity, to cover the fixed displacement of 0.1 mm. The corresponding time for a transverse phonon is 35 nsec. The measurement of the time-resolved signal from 0.8-THz phonons was made with a 100-nsec gate. It should take, accordingly, 136 nsec for a signal from ballistic phonons to reach its maximum value. The fact that the signal from 0.8-THz phonons re-

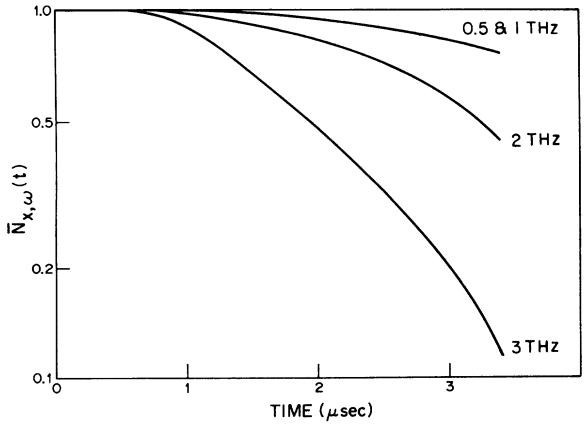

FIG. 3. Temporal evolution as observed in an integrating volume immediately behind the film-crystal interface $\bar{N}_{x,\omega}(t)$.

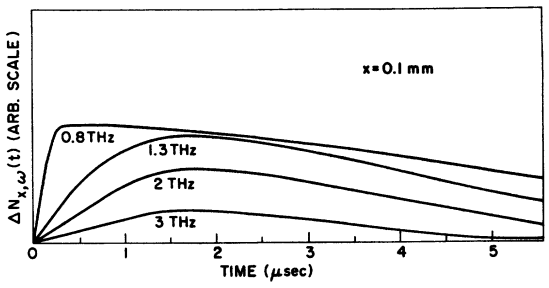

FIG. 4. Temporal evolution as observed in the focal volume $N_{x,\omega}(t)$. The focal volume is placed 0.1 mm behind the film-crystal interface.

quires nearly 300 nsec to reach a maximum confirms the earlier contention that even at this frequency the transport mechanism is not purely ballistic but must also involve a component of low-number scattering events. The 0.8 THz phonons should be expected to leave the observation volume at about the same rate at which they enter it. The observation that the signal amplitude decreases at a much slower rate is a reflection of the fact that the high-frequency phonons, which are congregated in the volume near the interface, decay into 0.8 THz, and other lower-frequency phonons, at a relaxation rate of the order of microseconds.

As should be expected from the results of Sec. III B, the signal from the higher-frequency phonons is more consistent with diffusive flow. Neglecting for the moment phonon decay, pure diffusive flow would require that the maximum in the time-resolved signal vary inversely with the diffusion constant. That is, the higher the phonon frequency, the longer the time to reach the maximum. The maximum in the time-resolved amplitude, calculated using Eq. (1) and the diffusion coefficients of Table I, is predicted to occur at 5.5, 12.5, and 56 μsec for 1-, 2-, and 3-THz phonons, respectively. These values must be corrected for the effect of phonon relaxation. In the same spirit as the approximation used in Sec. III C, we assume that for each phonon frequency there exists an effective single relaxation time $\tau_R(\omega)$ such that the observed time-resolved signal can be obtained by multiplying Eq. (1) by e^{-t/τ_R}. The τ_R required to obtain the maxima at the times shown in Fig. 4 are 5, 4, and 3 μsec for 1-, 2-, and 3-THz phonons, respectively.

IV. FURTHER DISCUSSION

Recent measurements in ruby place the lifetime of 29-cm^{-1} (0.87-THz) phonons at 0.5 μsec.[9] In this case, it is argued that the dominant decay mode is the three-phonon anharmonic process $l \rightarrow l + t$,[10] for which theoretical estimates of the lifetime by Orbach and Vredevoe[11] and by Klemens[12] are $\sim 5\times10^{-8}$ and $\sim 2\times10^{-7}$ sec, respectively. The corresponding lifetimes predicted for 3-THz phonons are $\sim 2\times10^{-10}$ and $\sim 7\times10^{-10}$ sec, respectively. It is interesting to determine why these lifetimes are not observed in the current experiment.

In a broadband phonon distribution the above decay mode is dominant in any one frequency interval only if the phonons in the interval are longitudinally polarized, and if the generation rate of phonons into the interval does not exceed the decay rate. Neither the phonons in SrF_2:Eu^{2+} nor those in ruby are exclusively longitudinally polarized. However, in both cases scattering at the probe ions is expected to result in mode conversion so that the otherwise longer-lived transverse phonons[11,13] cannot persist in time.

It has already been pointed out in Sec. III C that in the present experiment after 1 μsec the sum of all phonons of frequency greater than 3.5 THz is less than those in the 3-THz observation interval. Accordingly, after this time the generation of phonons into the 3-THz interval from "above" is small. The decay of 3-THz longitudinal phonons out of the interval will now be the dominant process providing the rate of generation into the 3-THz interval, through the combination of one or more low-frequency phonons, i.e., from "below," does not exceed the decay rate. In the analogous situation in the ruby experiments, the phonon population above and below the 0.87-THz interval is either kept artificially small by selective diffusion out of the observation volume[14] and/or by selective excitation.[9]

The phonon distribution in the present experiment differs from that in the ruby case when the input power into the heater is 5×10^3 W/mm^2. It can already be inferred from the results of Ref. 1 that although the spectral distribution function roughly resembles a Bose-Einstein distribution at $T \approx 13\,^\circ$K that, at least initially, the spectral energy density far exceeds that expected from a 13-$^\circ$K distribution. A numerical value for the phonon density present during the experimental observation can be estimated as follows. We determine the concentration of phonons in a given frequency interval from the spectral distribution function as shown in Fig. 4 of Ref. 1. For simplicity, we assume a Debye density of states and renormalize to the total input power as is done in Ref. 1. From Fig. 2 above we note that after 1 μsec the average distance traveled by phonons of 1–3 THz frequency is roughly 0.2 mm (presumably in any direction). Transport across the 1-mm^2 interface area occurs for the 20-nsec duration of the voltage pulse through the heater. Accordingly, the spectral energy flux is equivalent to a phonon density near the interface of 6×10^6, 6×10^5, and 3.4×10^4 mm^{-3}Hz^{-1} for 1-, 2-, and 3-THz phonons, respectively. The corresponding values for a Debye solid at equilibrium at 13 $^\circ$K is 10^3, 10^2, and 5.7 mm^{-3}Hz^{-1}.[15]

From the above it is clear that, although the spectral distribution resembles that of a 13 $^\circ$K Bose-Einstein distribution, the mode temperature, i.e., the number of phonons per unit frequency interval, is much higher than the one obtained at equilibrium. If the phonon pulse were completely isolated within the observation volume the ratio of high-to-low frequency phonons would increase

as the distribution tends toward an equilibrium temperature which would be higher than 13 °K. In other words, the dominant process would be the combination of low-frequency phonons to form high-frequency phonons. The injected phonon distribution is not isolated in the observation volume but, in fact, can progress into the remainder of the crystal, and ultimately come to equilibrium with the helium bath. In order to reach equilibrium at 13 °K, however, the phonon concentration would have to be diluted by a factor of roughly 10^{-3}. This would require an expansion into a volume bounded by surfaces roughly 2 mm in all directions from the interface which, from the results of Sec. III B, would take of the order of milliseconds to achieve. Accordingly, during the initial interval of the order of microseconds the production of phonons into the 3-THz interval from below is still an important contributing process. The pertinent three- and four-phonon processes have relaxation rates which can be of the order of microseconds.[11,13] We conclude that it is these processes which are dominant in determining the observed relaxation times.

Recombination of low-frequency phonons is among the possible causes of the deviations from the Gaussian diffusion profiles noted in Sec. III B. Since these phonons can penetrate into the crystal more readily than high-frequency phonons, they can by recombination increase the high-frequency concentration in the tails of the profile. Neither the relative importance of this effect, of phonon-focusing, of low-number scattering, nor that of others has been considered in detail here.

V. CONCLUSION

We have demonstrated that the vibronic sideband spectrometer can be used to experimentally determine the evolution of a phonon distribution in the four-dimensional space of phonon density, frequency, space, and time. Many of the complexities are observed which are expected in the evolution of a broad phonon distribution propagating in this space. In principle, it is now possible to compare the experimentally determined transport properties of a phonon distribution with the theoretical predictions formulated by Kwok.[16] We prefer instead to turn our attention to the transport behavior of originally nearly monochromatic phonon distributions. The result of the first experiment along these lines is to be reported on in the near future.

ACKNOWLEDGMENT

The authors acknowledge helpful discussions with W. L. Schaich.

---

*Work supported by NSF Grant Nos. 72-03070 and 76-23571. One of the authors (W.G.) acknowledges a travel grant from the Deutsche Forschungsgemeinschaft.

[1]W. E. Bron and W. Grill, Phys. Rev. B 16, 5303 (1977) (preceding paper).

[2]See, e.g., C. H. Anderson and E. Sabisky, in *Physical Acoustics*, edited by W. P. Mason and R. N. Thurston (Academic, New York, 1971), Vol. VIII; M. J. Colles and J. A. Giordmaine, Phys. Rev. Lett. 27, 670 (1971); J. Shah, R. F. Leheny, and A. H. Dayem, *ibid*. 33, 818 (1974).

[3]W. E. Bron and F. Keilmann, Phys. Rev. B 12, 2496 (1975).

[4]R. C. Dynes and V. Narayanamurti, Phys. Rev. B 6, 143 (1972).

[5]See, e.g., P. G. Klemens, in *Solid State Physics*, edited by F. Seitz and D. Turnbull (Academic, New York, 1958), Vol. VII.

[6]See, e.g., R. J. von Gutfeld, *Physical Acoustics*, edited by W. P. Mason (Academic, New York, 1968), Vol. V.

[7]Equation (1) can be readily derived from the three-dimensional diffusion relations which appear in S. Chandrasekhar, Rev. Mod. Phys. 15, 1 (1943).

[8]The corresponding times for 2- and 1-THz phonons is 1.2 and 0.7 μsec, respectively.

[9]R. S. Meltzer and J. E. Rives, Phys. Rev. Lett. 38, 421 (1977); K. F. Renk (private communication).

[10]l, t stand for the longitudinal and transverse phonon branches, respectively.

[11]R. Orbach and L. A. Vredevoe, Physics (N.Y.) 1, 91 (1964).

[12]P. G. Klemens, J. Appl. Phys. 38, 4573 (1967).

[13]P. C. Kwok and P. B. Miller, Phys. Rev. 146, 592 (1966).

[14]K. F. Renk and J. Peckenzell, J. Phys. (Paris) 33, C4-103 (1972).

[15]In calculating the Debye density of states we assume the phonon velocity to be the weighted-average acoustic velocity.

[16]P. C. Kwok, Phys. Rev. 175, 1208 (1968).